

## **THE EFFECTIVENESS OF LIGHT INTERVENTIONS OF ANTI-SEISMIC REINFORCEMENTS ON A MASONRY BUILDING**

**Sandro CHIOSTRINI<sup>1</sup>, Luca FACCHINI<sup>2</sup> And Andrea VIGNOLI<sup>3</sup>**

### **SUMMARY**

Light anti-seismic upgrade is widely used in practice, although a precise theoretical model for the masonry behaviour is extremely difficult to set up. Therefore, an exact prediction of the effectiveness of upgrade interventions becomes extremely hard.

The aim of this work is to evaluate such effectiveness on a masonry building in Rometta, a village in the Apennine Mountains of central Italy. The building was damaged by the earthquake of October 10<sup>th</sup>, 1995, which took place in Lunigiana and Garfagnana, two nearby valleys in the Apennine.

### **INTRODUCTION**

The effectiveness of light interventions of anti-seismic upgrade on masonry structures is usually hard to predict owing to the uncertainties of the building materials, which are usually heterogeneous and anisotropic.

In this paper a masonry building in the Apennine mountains was taken into consideration, which was damaged during the earthquake of October 10<sup>th</sup>, 1995; the building was upgraded by means of the insertion of steel bars in the upper part of the masonry walls, following the regulations of Tuscany region contained in the Ministerial Decree of December 29<sup>th</sup>, 1995.

#### **The study was conducted in two main phases:**

1. A campaign of dynamic measurements was carried out: the accelerations of determined locations of the structure were measured under traffic load, ambient vibrations, and vibrations induced by a road roller driven over a wooden step, which simulated a pulse noise.
2. The measurements were subsequently numerically analysed and the main frequencies of the structure were evaluated.

Such analyses were carried out before and after the upgrade intervention.

### **DESCRIPTION OF THE BUILDING**

The building into consideration consists of a masonry structure on three main levels, a ground level, first and second floor. The first part was built in 1918, and later on (about 1966-67) extended to the present dimensions.

Such reconstruction of the temporal evolution of the building implies many approximations, due to the house not being of outstanding historical interest, and the consequent difficulty to find historical documents about the house itself.

<sup>1</sup> Department of Civil Engineering, University of Florence, Florence, Italy Email: schio@dicea.unifi.it

<sup>2</sup> Department of Civil Engineering, University of Florence, Florence, Italy Email: luca@dicea.unifi.it

<sup>3</sup> Department of Civil Engineering, University of Florence, Florence, Italy.

The building, before the intervention, showed acceptable safety levels with the exception of the second floor of the central part, which was affected by severe damages due to a scarce link between concurrent walls. Such lesions were vertically oriented in correspondence of the conjunction of two walls, and were diagonally oriented on the architrave of windows and doors.

The intervention consisted mainly in the insertion of steel bars in the upper part of the masonry walls of the second floor, as indicated in Fig. 3.

## TEST METHODOLOGY

The most useful tests performed on the structure were realised by means of a road roller falling from a wooden step (see Fig. 2).

Figures 2 and 3 show the locations and directions of the employed accelerometers; they were disposed according to the two main directions of the building.

The records of accelerations were carried out at a sampling frequency of 250 Hz, for a total time of 20 s. Before the analog/digital converter, an anti-aliasing analog filter was implemented, with a cut-off frequency of 50 Hz.



**Fig. 1: the road roller in front of the wooden step; on the left of the step an accelerometer can be seen.**

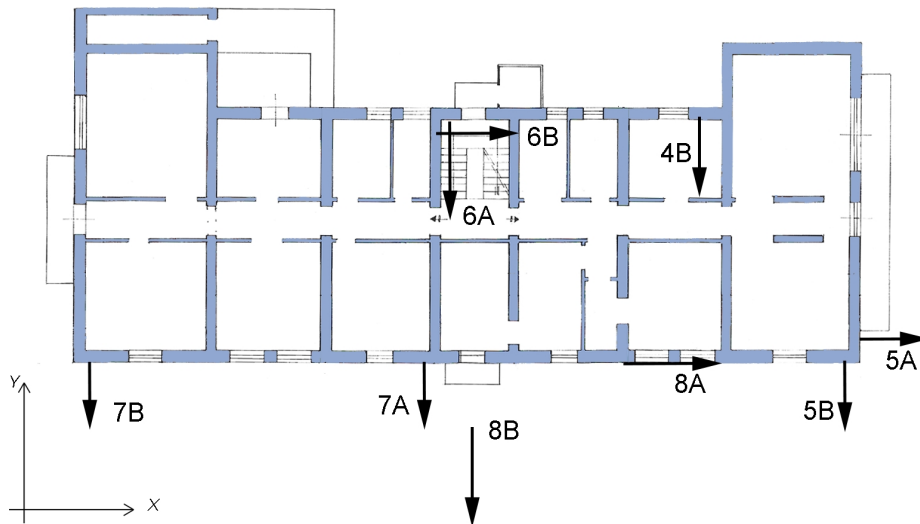


**Fig. 2: arrangement of accelerometers at the first floor level; accelerometer n. 8B records the pulse from the road roller and is located at ground level, on the public street.**

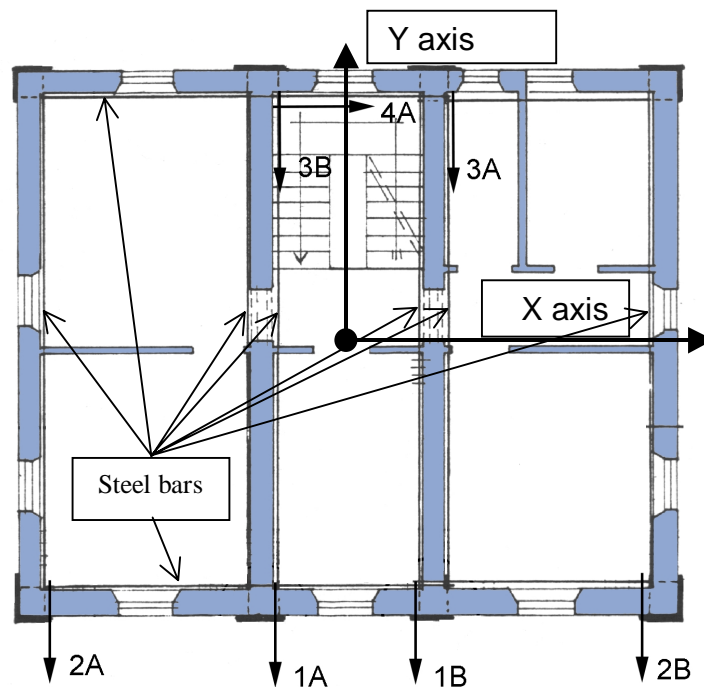


**Fig. 3: the arrangement of accelerometers at the second floor level; the reference system for the second floor is also indicated.**

### DATA PROCESSING

Recorded data were successively processed by means of a PC computer. A first model was set up in order to identify the possible eigenshapes; the model was based on the hypothesis that the floors were infinitely rigid in their plane; such hypothesis can be acceptable for the second floor, whose ground plan is approximately square, and the floors are strong enough (especially after the upgrade intervention), but it is actually hard to accept for

the first floor; nevertheless, it can at least provide a comparison for the eigenshapes of the structure which have been evaluated by means of the computer program, and that's mainly why it was first introduced.

Moreover, the hypothesis of small displacements, velocities and accelerations was introduced: this is a far more acceptable hypothesis, as it can be verified *a posteriori* on the recorded accelerograms.

From these two hypotheses, it steams out that the (vector) acceleration of a given point of the structure can be expressed in terms of the acceleration of its centre of mass, and the angular acceleration; in fact, from the rigid-body equation of motion (in terms of velocities)

$$\mathbf{v}_{P_k} = \mathbf{v}_C + \boldsymbol{\omega} \wedge (P_k - C) \quad (1)$$

where  $P_k$  indicates the location of the  $k$ -th accelerometer (in the reference system indicated in Fig. 3),  $\mathbf{v}$  is the velocity vector, and  $\boldsymbol{\omega}$  the angular velocity of the floor; upon derivation with respect to time, and neglecting the derivative of the position vector  $(P_k - C)$ , the following expression for the acceleration of  $P_k$  is obtained:

$$\mathbf{a}_{P_k} = \mathbf{a}_C + \dot{\boldsymbol{\omega}} \wedge (P_k - C) \quad (2)$$

In the case that the positive direction of the accelerometer located at  $P_k$  is indicated by the versor  $\mathbf{v}_k$ , the measurement of the  $k$ -th accelerometer will be:

$$a_k = \mathbf{v}_k \cdot \mathbf{a}_{P_k} = \mathbf{v}_k \cdot [\mathbf{a}_C + \dot{\boldsymbol{\omega}} \wedge (P_k - C)] \quad (3)$$

where the dot stands for the scalar product. In particular, if  $\alpha_k$  is the angle of the versor  $\mathbf{v}_k$  with the positive direction of the  $x$ -axis, it can be obtained that

$$a_k = (a_{Cx} - \dot{\omega}(y_{P_k} - y_C)) \cos \alpha_k + (a_{Cy} + \dot{\omega}(x_{P_k} - x_C)) \sin \alpha_k \quad (4)$$

In the preceding formula (4),  $x$  and  $y$  indicate the co-ordinates of the desired point in the global reference system; in such a way, it is possible to express all the measured accelerations as functions of the accelerations of the three degrees of freedom of each floor (which can be indicated as the vector  $[a_{Cxh} \ a_{Cyh} \ \dot{\omega}_h]^t$ , where  $h$  indicates the  $h$ -th floor): a matrix is then obtained that relates the global vector of the accelerations of all the floors of the structure and the accelerations of the measured locations:

$$\mathbf{A} \mathbf{a}_{dof} = \mathbf{a}_{meas} \quad (5)$$

where  $\mathbf{a}_{dof} = [a_{Cx_1} \ a_{Cy_1} \ \dot{\omega}_1 \ \cdots \ a_{Cx_h} \ a_{Cy_h} \ \dot{\omega}_h \ \cdots \ a_{Cx_N} \ a_{Cy_N} \ \dot{\omega}_N]^t$  is a vector whose components are the accelerations of the degrees of freedom of the structure (whose floors are supposed infinitely rigid in their plane) and  $\mathbf{a}_{meas} = [a_1 \ \cdots \ a_k \ \cdots \ a_M]^t$  is the vector of all the measured accelerations. In this way, the spectral density tensors are related by:

$$\mathbf{A} \mathbf{S}_{A_{dof} A_{dof}}(f) \mathbf{A}^t = \mathbf{S}_{A_{meas} A_{meas}}(f) \quad (6)$$

where  $\mathbf{S}_{A_{dof} A_{dof}}(f)$  and  $\mathbf{S}_{A_{meas} A_{meas}}(f)$  are, respectively, the evolutionary spectral tensors of the accelerations of the degrees of freedom and of the measured accelerations.

For each frequency  $f$ , equation (6) is actually an overdetermined set of  $M$  linear equations whose unknowns are the components of the spectral tensor  $\mathbf{S}_{A_{dof} A_{dof}}(f)$ : such set can be solved by means of the pseudo-inverse of the matrix  $\mathbf{A}$  in the following way:

$$\mathbf{S}_{A_{dof} A_{dof}}(f) = (\mathbf{A}^t \mathbf{A})^{-1} \mathbf{A}^t \mathbf{S}_{A_{meas} A_{meas}}(f) \mathbf{A} (\mathbf{A}^t \mathbf{A})^{-1} \quad (7)$$

In the preceding equation no. 7, the spectral tensor  $\mathbf{S}_{A_{dof} A_{dof}}(f)$  depends on the position of the point  $C$ , which is the reference for the evaluation of the spectral densities of the rigid plane accelerations; for a more complete description of such accelerations and movements, it would be advisable to choose the point  $C$  in correspondence of the stiffness centre, namely the centre of rotation of the second floor.

In order to evaluate such position from the spectral tensor  $\mathbf{S}_{A_{dof} A_{dof}}(f)$ , it might be noticed that if it is evaluated with respect to the stiffness centre, then the accelerations along the principal axis (i.e. the translational accelerations of the second floor) should be minimised, and so also their spectral densities should show a minimum variance.

Following this criterion, the variances of the translational accelerations were evaluated for different positions of the point  $C$ , and the position of  $C$ , which minimised their sum, was found by means of a neural network interpolation.

In the following Fig. 4 and Fig. 5, the origin of the axis coincides with the geometric centre of the second floor, as indicated in Fig. 3, and the position of the stiffness centre is expressed in metres.

In the contour plots (on the right side of Fig. 4 and Fig. 5) the position of  $C$  which minimises the sum of the variances of the translational accelerations is outlined by a black point.

Before the upgrade intervention, such position resulted  $C = [3.6959 \quad -0.9377]$  metres.

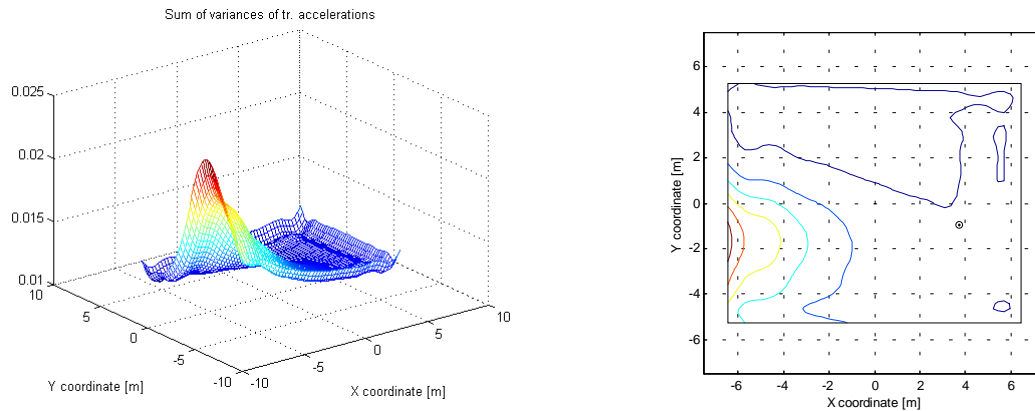


**Fig. 4: three-dimensional plot (left) and contour plot (right) of the sum of translational accelerations variances with respect to position of the centre  $C$  in the reference system of Fig. 3 – before the upgrade intervention**

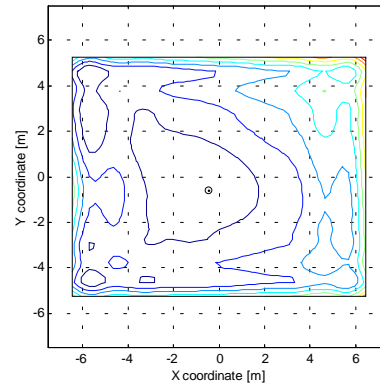


**Fig. 5: three-dimensional plot (left) and contour plot (right) of the sum of translational accelerations variances with respect to position of the centre  $C$  – after the upgrade intervention**

After the upgrade intervention, the position of the stiffness centre resulted  $C = [-0.4446 \quad -0.5765]$  metres.

As it is clear from a first comparison between Fig. 4 and Fig. 5, the stiffness centre after the upgrade intervention is much more near to the geometric centre of the floor: this is in accordance with the overall stiffness distribution of the structure, and it remarks that, thanks to the upgrade, the floor behaviour is much more similar to a rigid plane than before.

### FURTHER RESULTS OF DYNAMIC TESTS

After the position of the stiffness centre was determined in the reported way, the spectral tensor of the rigid plane accelerations were evaluated following the procedure of paragraph 4.

The above-described analysis was carried out for the upper level of the building, as the hypothesis of a rigid plane followed the actual behaviour more strictly.

#### Tests carried out before the upgrade intervention

The following figures show the spectral densities of the rigid plane accelerations recorded before the upgrade intervention.

The structural frequencies, which arise from the data processing for the  $x$ ,  $y$  directions and the rotational accelerations, are respectively 5.6152 Hz, 6.3477 Hz and 8.0566 Hz.

The power spectral densities of Fig. 6 are obtained by means of the recorded accelerations of 1A, 1B, 2A, 2B, 3A, 3B and 4A accelerometers.

In the following Fig. 6 and Fig. 7 the spectral tensor is reported in this way: on the main diagonal, the transfer functions for each acceleration ( $x$ ,  $y$  and rotational, respectively) are indicated; below the main diagonal the phase angles between such accelerations are indicated, and over the main diagonal the coherence functions are reported.

The first, second and third signals are respectively the  $x$  and  $y$  accelerations and the rotational acceleration.

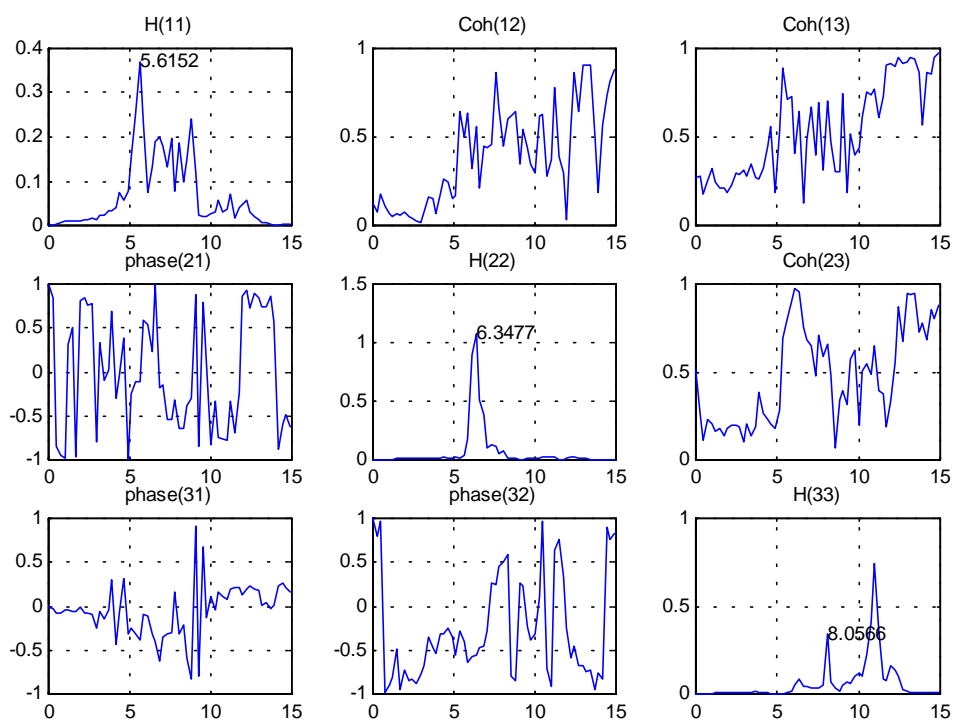


**Fig. 6: spectral tensor of rigid plane accelerations of the second floor before the upgrade intervention.**

### Tests carried out after the upgrade intervention

As mentioned earlier, the upgrade consisted in the insertion of steel bars in the masonry walls; the instruments were placed in the same locations as before, in order to obtain a comparison on the structural frequencies.

The structural frequencies which arise from the data processing for the  $x$ ,  $y$  directions and the rotational accelerations are respectively 6.1035 Hz, 6.8359 Hz and 9.2773 Hz; in other words, the upgrade intervention brought an overall increase of the structural frequencies.

It can also be noticed that the transfer functions of the accelerations are now more regular than before the upgrade, and this indicates that the overall behaviour of the second floor is more similar to a rigid plane.

### CONCLUSIONS

An overall increase of the main structural frequency was reported for the translational and rotational accelerations of the second floor.

Respectively, such frequencies increased by 8.70%, 7.69% and 15.15%.

The inserted steel bars were actually much more along the  $y$  direction than in the other; moreover, the steel bars in the transversal direction could be placed on both faces of the masonry walls, while in the other direction the bars could be placed on one side only of the walls.

The change of the shape of the power spectral density (namely, a regularisation) can be interpreted as a capability of the rigid plane hypothesis to follow the actual situation; in other words, this means that the steel bars were undoubtedly a reinforcement which stiffened the floors of the building, with consequent overall benefit.

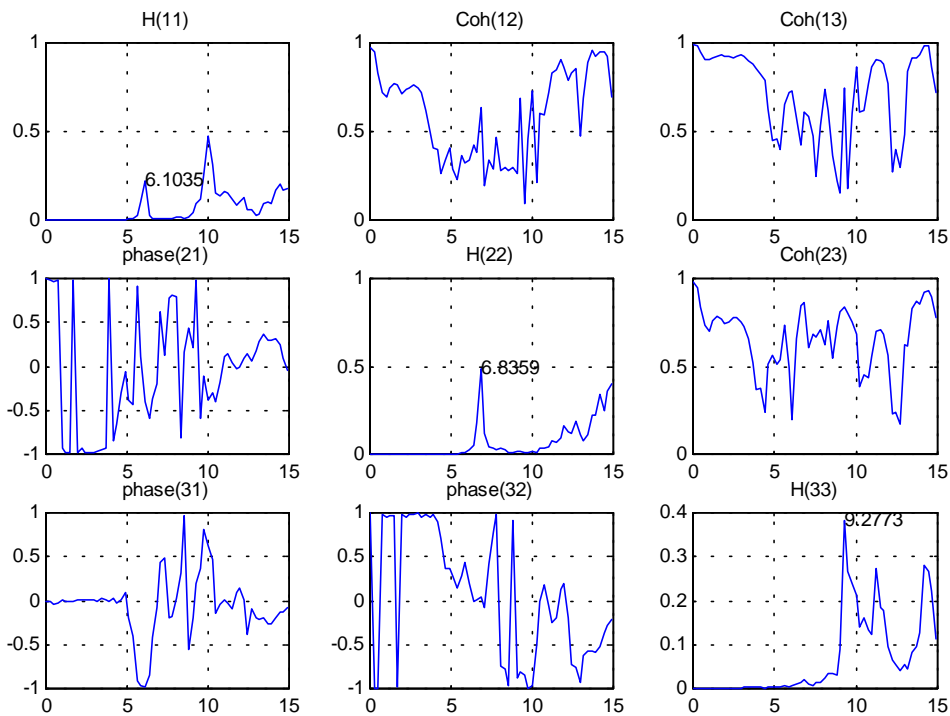


**Fig. 7: spectral tensor of rigid plane accelerations of the second floor after the intervention.**

#### ACKNOWLEDGEMENTS

The accelerations measurements were carried out by Italian Seismic Service, and subsequently made available by means of the Tuscany Region: both are gratefully acknowledged. Italian Ministry for University and Scientific Research financial aid is also gratefully acknowledged.

#### REFERENCES

1. A.Pavese, Indagine sperimentale e numerica su un prototipo di edificio in Muratura: studi sui risultati della caratterizzazione dinamica, Atti 8o convegno Nazionale ANIDIS L'Ingegneria Sismica in Italia, Taormina, 21-24 settembre 1997 pp.1049-1056.
2. J.Bendat, Allan G. Piersol, Random Data: Analysis and Measurement Procedures, Wiley-Interscience, 1971.
3. B. Gold, C.M. Rader, Digital Processing of Signals, McGraw Hill Book Company, 1969.
4. Kennet G. McConnell, Vibration Testing. Theory and Practice, John Wiley & Sons, Inc., New York, 1995.
5. Donald B. Percival and Andrew T. Walden, Spectral Analysis for Physical Applications, Cambridge, 1993
6. T.T.Soong, Mircea Grigoriu, Random Vibration of Mechanical and structural systems PTR Prentice Hall Englewood Cliffs, New Jersey 07632, 1993.